

# Intra-Ophthalmic Artery Chemotherapy Triggers Vascular Toxicity through Endothelial Cell Inflammation and Leukostasis

Jena J. Steinle,<sup>1,2</sup> Qiubua Zhang,<sup>1</sup> Karin Emmons Thompson,<sup>3</sup> Jordan Toutouchian,<sup>3</sup> C. Ryan Yates,<sup>3</sup> Carl Soderland,<sup>4</sup> Fan Wang,<sup>5</sup> Clinton F. Stewart,<sup>5</sup> Barrett G. Haik,<sup>1,6</sup> J. Scott Williams,<sup>7</sup> J. Scott Jackson,<sup>8</sup> Timothy D. Mandrell,<sup>8</sup> Dianna Johnson,<sup>1,2</sup> and Matthew W. Wilson<sup>1,6,9</sup>

**PURPOSE.** Super-selective intra-ophthalmic artery chemotherapy (SSIOAC) is an eye-targeted drug-delivery strategy to treat retinoblastoma, the most prevalent primary ocular malignancy in children. Unfortunately, recent clinical reports associate adverse vascular toxicities with SSIOAC using melphalan, the most commonly used chemotherapeutic.

**METHODS.** To explore reasons for the unexpected vascular toxicities, we examined the effects of melphalan, as well as carboplatin (another chemotherapeutic used with retinoblastoma), in vitro using primary human retinal endothelial cells, and in vivo using a non-human primate model, which allowed us to monitor the retina in real time during SSIOAC.

**RESULTS.** Both melphalan and carboplatin triggered human retinal endothelial cell migration, proliferation, apoptosis, and increased expression of adhesion proteins intracellular adhesion molecule-1 [ICAM-1] and soluble chemotactic factors (IL-8). Melphalan increased monocytic adhesion to human retinal endothelial cells. Consistent with these in vitro findings, histopathology showed vessel wall endothelial cell changes, leukostasis, and vessel occlusion.

**CONCLUSIONS.** These results reflect a direct interaction of chemotherapeutic drugs with both the vascular endothelium and monocytes. The vascular toxicity may be related to the pH, the pulsatile delivery, or the chemotherapeutic drugs used. Our long-term goal is to determine if changes in the drug of choice

and/or delivery procedures will decrease vascular toxicity and lead to better eye-targeted treatment strategies. (*Invest Ophthalmol Vis Sci.* 2012;53:2439-2445) DOI:10.1167/iovs.12-9466

Retinoblastoma is the most common primary intraocular malignancy in children. When retinoblastoma is confined to the eye, cure rates exceed 90%. While multiple treatment modalities are available, there has been a recent focus on performing targeted vascular drug delivery via super-selective intra-ophthalmic artery chemotherapy (SSIOAC) infusion, with melphalan as the drug most commonly used.<sup>1,2</sup> Selective delivery of chemotherapy to organ-limited tumors should provide effective concentrations of appropriate drugs where needed while reducing systemic exposure, and SSIOAC has been very successful in doing so.<sup>1,2</sup>

Yet the ultimate success of targeted vascular drug delivery will depend upon the ability of the vascular system to remain functionally intact to adequately distribute the drug throughout treatment, as well as to sustain any remaining healthy tissue after tumor cells have been therapeutically destroyed. Melphalan is cytotoxic through the formation of intrastrand DNA cross-links or DNA-protein cross-links via the two chloroethyl groups on the molecule, resulting in alkylation.<sup>3</sup> While initial reports detailed the efficacy of SSIOAC with melphalan in the treatment of retinoblastoma with minimal problems,<sup>1,2</sup> more recent studies have reported vascular toxicities such as ophthalmic artery thrombosis, sectoral choroidal nonperfusion, as well as retinal and vitreous hemorrhages.<sup>4-6</sup> These vascular toxicities may result from overdose of the chemotherapeutic. For instance, previous studies have determined that 4 µg/mL melphalan is 100% cytotoxic to primary retinoblastoma cells in culture,<sup>7</sup> meanwhile clinically, 30 mL of 167 µg/mL melphalan is infused during SSIOAC<sup>4,6</sup>; the actual concentration that enters the eye is unknown.

As part of a group of parallel studies using primary human retinal endothelial cells and a newly developed in vivo non-human primate (NHP) model to determine if SSIOAC can be improved to obviate vascular side effects and provide needed treatment with appropriate drugs, we report on cellular activity as a result of exposure to clinically used chemotherapeutics and preliminary histopathology post SSIOAC.

## METHODS

### In Vitro Studies

Primary human retinal microvascular endothelial cells (REC, lot 181) were obtained from Cell Systems Corp. (CSC, Kirkland, WA). Cells

From the Departments of <sup>1</sup>Ophthalmology, <sup>2</sup>Anatomy and Neurobiology, <sup>3</sup>Pharmaceutical Sciences, <sup>7</sup>Radiology, and <sup>8</sup>Comparative Medicine, University of Tennessee Health Science Center, Memphis, Tennessee; <sup>4</sup>Cell Systems Corporation, Kirkland, Washington; and the Departments of <sup>5</sup>Pharmaceutical Sciences, <sup>6</sup>Surgery, Division of Ophthalmology and <sup>9</sup>Pathology, St. Jude Children's Research Hospital, Memphis, Tennessee.

Supported by an unrestricted grant to the Department of Ophthalmology from Research to Prevent Blindness, New York, New York; National Eye Institute Vision Core grants, numbers PHS 3P30, EY013080 (DJ); an unrestricted grant from the St. Giles Foundation to MWW; and grants (CA23099, CA21765) from the American Lebanese Syrian Associated Charities to CFS and FW.

Submitted for publication January 10, 2012; revised March 1, 2012; accepted March 3, 2012.

Disclosure: J.J. Steinle, None; Q. Zhang, None; K. Emmons Thompson, None; J. Toutouchian, None; C.R. Yates, None; C. Soderland, Cell Systems Corp (I, E); F. Wang, None; C.F. Stewart, None; B.G. Haik, None; J.S. Williams, None; J.S. Jackson, None; T.D. Mandrell, None; D. Johnson, None; M.W. Wilson, None

Corresponding author: Jena J. Steinle, Hamilton Eye Institute, University of Tennessee Health Science Center, 930 Madison Avenue, 7th Floor, Memphis, TN 38163; jstein11@uthsc.edu.

were grown in M131 medium containing microvascular growth supplements, 10  $\mu\text{g}/\text{mL}$  gentamicin, and 0.25  $\mu\text{g}/\text{mL}$  amphotericin B (Invitrogen, Carlsbad, CA). Before the experiment, cells were transferred to high (25 mM) glucose medium (CSC), supplemented with antibiotics, and grown to 80% confluence. Primary cells (passages 2–4) were used. Cells were quiesced by incubating in high glucose medium without fetal bovine serum (FBS) for 24 hours, then used to perform the experiments unless otherwise indicated. Once confluent, cells were trypsinized and counted using hemocytometry.

Treatment drug solutions were made according to the manufacturer's directions and added at the following doses, unless otherwise indicated—melphalan: 0.1  $\mu\text{g}/\text{mL}$ , 0.4  $\mu\text{g}/\text{mL}$ , 1.0  $\mu\text{g}/\text{mL}$ , and 4.0  $\mu\text{g}/\text{mL}$  (100% cytotoxic in cell culture<sup>7</sup>; Bioniche Pharma, Lake Forest, IL); carboplatin: 10.0  $\mu\text{M}$ , 100.0  $\mu\text{M}$ , and 1.0 mM (concentrations of 2.0 nM to 200.0  $\mu\text{M}$  were found to reduce cell viability and proliferation<sup>8</sup>; APP, Schaumburg, IL). Treatment with sterile drug diluent (provided by the manufacturer for melphalan [containing sodium citrate 0.2 g, propylene glycol 6.0 mL, ethanol (96%) 0.52 mL, and water for injection to a total of 10 mL], and normal saline for carboplatin) was used as a control. Data from each treatment group, presented as a percentage of control, were compared with the control group. Statistics were performed using Prism v4.0 software (GraphPad Software, La Jolla, CA) using a Kruskal-Wallis test and Dunn's posttest, assuming statistical significance at  $P < 0.05$ .

To measure treatment-induced cell death (apoptosis) using ELISA (a photometric enzyme immunoassay that quantitates cytoplasmic histone-associated DNA fragments [mono- and oligonucleosomes] after induced cell death), we placed an equal number of cells into each well of 24-well plates and cultured in high glucose medium for 3 days. Cells were then starved (without growth factor) overnight, followed by treatment for 24 hours. Briefly, according to instructions supplied with the Cell Death Detection ELISA kit (Roche Applied Science, Indianapolis, IN), the cells were washed with PBS, lysed, and the lysates collected and incubated with immunoreagent (antihistone and anti-DNA, provided in the kit). The resultant antibody-nucleosome complexes were measured spectrophotometrically at 405 nm (vs. 490-nm reference). Absorption (recorded as optical density) at 405 nm increased with increasing presence of cytoplasmic DNA fragments in the lysate (specifically histones H1, H2A, H2B, H3, and H4).

We used the BD Biocoat Angiogenesis Assay (BD Biosciences, Bedford, MA) to test how treatment affected cell migration. The angiogenesis assay works well for migration studies because the porous, fluorescence-blocking inserts allow for movement (migration) of cells from one level to another within the same well. Since the insert blocks the passage of light from 490 to 700 nm, only fluorescence from cells that have migrated is counted and correlated to cell number. Briefly, 100,000 cells/well was added to the top three levels of 24-well angiogenesis plates. Treatments were added to the lower wells of each angiogenesis plate for 24 hours. After 24 hours, calcein AM, a fluorescence dye, was dissolved in Hank's buffered saline and placed into a new 24-well plate, which was combined with the angiogenesis system plate. After 1.5 hours, the plate was read on a fluorescent plate reader at 485 nm (vs. 530-nm reference).

To study how treatment affected proliferation, 50,000 cells were plated into each well of a 96-well dish and incubated for 24 hours. After a 48-hour treatment, the cellular proliferation was determined using tetrazolium salt WST-1 and a microplate reader according to the assay manufacturer's instructions (Cell Proliferation Assay Kit, WST dye, ELISA based; Millipore, Billerica, MA) at 440 nm. The absorbance at 440 nm (recorded in optical density) is directly correlated with cellular proliferation.

Those treatments producing significant cellular activity were used in microarray analyses to determine which genes were altered after 24-hour treatment. The chemotherapeutic was placed onto four 60-mm dishes of cells, and four dishes remained untreated as controls. After 24 hours, the RNA was collected and frozen at  $-80^{\circ}\text{C}$  for later analyses. Microarray analyses were done by Genome Explorations, Memphis, Tennessee, using their human Affymetrix gene chip. Genome

Explorations provided a list of differentially expressed genes with statistics and analyses of the enriched pathways in the differentially expressed genes. The data discussed in this publication have been deposited in NCBI's Gene Expression Omnibus and are accessible through GEO Series accession number GSE34389 (in the public domain).

ELISA analyses on treated REC for those proteins identified by microarray analysis were used to verify that increased RNA production resulted in increased protein production. ELISAs were performed according to the manufacturer's instructions (IL-8; Thermo Fisher, Pittsburgh, PA, and intracellular adhesion molecule-1 [ICAM-1]; Millipore). Briefly, as both the IL-8 and ICAM-1 are colorimetric ELISA assays, they are read on a standard microplate reader, with results given in optical density. The IL-8 assay uses a biotinylated antibody reagent and anti-human IL-8 labeling. The ICAM-1 assay uses anti-ICAM-1 labeling. Both IL-8 and ICAM-1 absorbances are measured at 450 nm (vs. 550-nm reference).

The exploratory nature of these studies led to the choice to examine the effects of melphalan, as the current drug of choice for SSIOAC, at the 100% cytotoxic dose of 4  $\mu\text{g}/\text{mL}$  on monocytic cell adhesion to REC. In a parallel-plate flow chamber with a continuous flow-loop and loaded with REC monolayers grown on slides (Cytodyne Inc., La Jolla, CA), at a shear stress of 2 dyne/cm,<sup>2,9,10</sup> U937 cells ( $2.5 \times 10^6$  cells/mL, ATCC, Manassas, VA) were perfused through the chamber in RPMI 1640 medium containing 10% serum. After 2 hours, the chemotherapeutic was injected into the flow chamber. Phase contrast images of U937 cells adhering to human REC monolayers were obtained using a Nikon Diaphot 300 phase-contrast inverted microscope (Nikon Instruments, Inc., Melville, NY) equipped with a Dage-MTI series 68 camera (Dage-MTI, Michigan City, IN). High-resolution video was directly captured and analyzed using Adobe Premier Pro CS5.5 (Adobe Systems, Inc., San Jose, CA). Adhesion events were monitored for up to 4 hours over 8 fields of view ( $\varnothing$  20 mm). Firm adhesion was defined as interacting monocytes remaining stationary for more than 3 seconds.<sup>11,12</sup>

Following flow chamber analysis, monolayer slides were fixed at room temperature with 4% formaldehyde for 10 minutes and washed with PBS three times. Human anti-ICAM-1 conjugated to PerCp-Cy5.5 and anti-P-selectin (Santa Cruz Biotechnology, Santa Cruz, CA) were diluted in PBS and incubated with the slide for 1 hour at room temperature. Slides were washed with PBS and incubated with DAPI nuclear stain for 10 minutes and washed again in PBS. Mounting medium and coverslips were added and sealed. Slides were maintained at  $4^{\circ}\text{C}$  until analysis. Slides were analyzed using a Zeiss LSM 710 confocal imaging system with Zen 2010 software (Carl Zeiss Microscopy, LLC, Thornwood, NY).

## Non-Human Primate Studies

Six adult male Rhesus macaques (9–13 kg, *Macacca mulatta*) were randomly assigned into one of two treatment cohorts ( $n = 3$  per cohort), melphalan (5 mg/mL) or carboplatin (30 mg/30 mL). These treatment doses are higher than those used in the cell-culture model but are consistent with those used to treat children.<sup>1,2,4,5,7</sup> This NHP model was chosen for three principle reasons. Rhesus macaques have (1) similar body size (weight of 13 kg and body surface area of 0.5 m<sup>2</sup>) to an average 2-year-old child, which is the likely age of a child undergoing treatment for retinoblastoma; (2) comparable orbital vascular anatomy (the ophthalmic artery is a first-order branch of the internal carotid); and (3) an eye with anatomy and size similar to that of a 2-year-old child (median size of eye at gross examination [19 mm  $\times$  19 mm  $\times$  19 mm as compared with child's eye of 20 mm  $\times$  20 mm  $\times$  20 mm], and vitreous cavity of approximately 5 cm<sup>3</sup>).

Animals were followed daily, post SSIOAC, by veterinarians for complications related to anesthesia and SSIOAC. Activity, diet, and blood counts were monitored. Weekly ophthalmic examinations were performed under intramuscular ketamine (10 mg/kg) sedation. Digital external and retinal images were obtained (data published previously<sup>6</sup>).

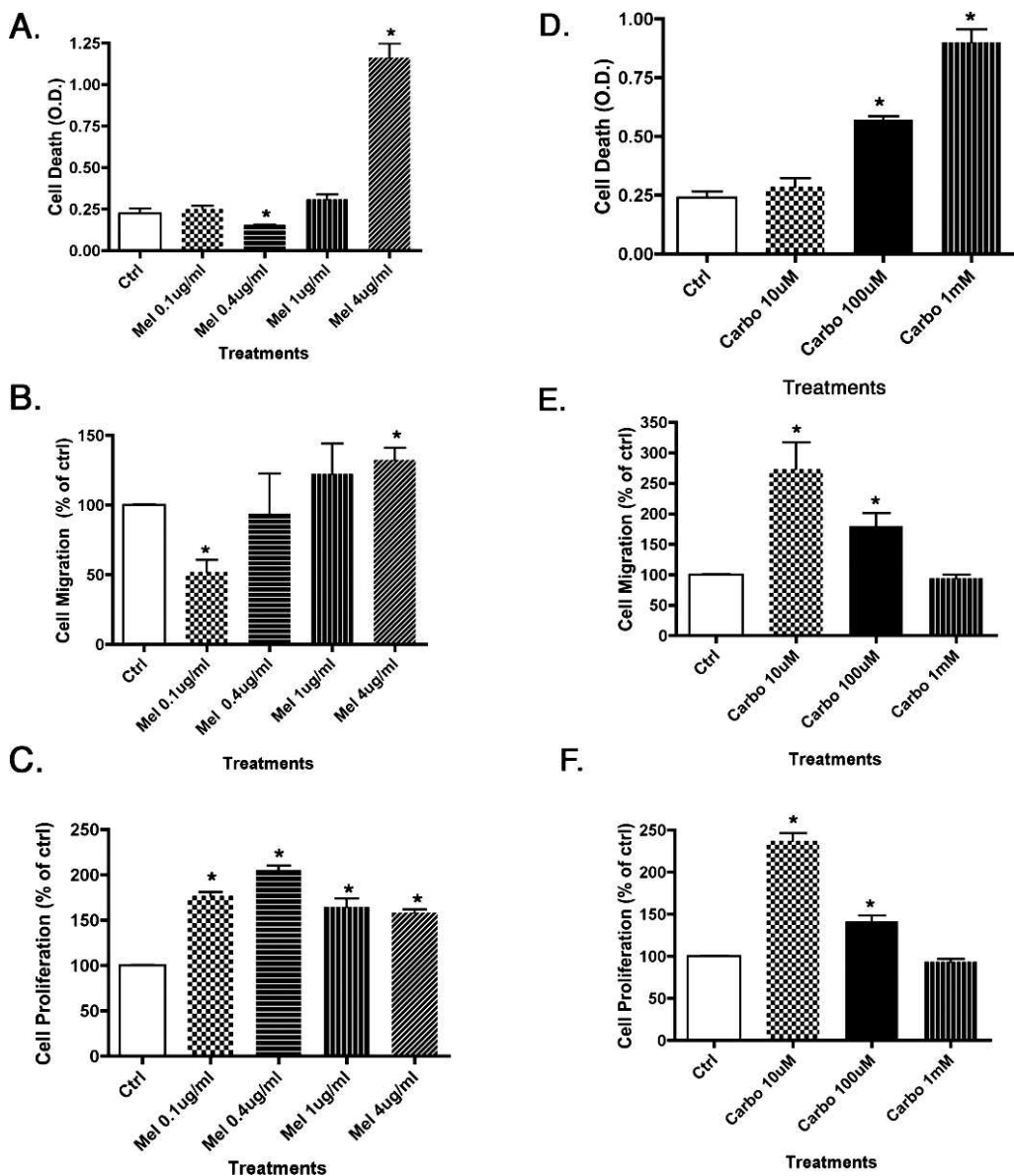


**FIGURE 1.** The mean (percentage of control) and SEM of retinal endothelial cells either left untreated (control) or treated with escalating doses ( $n = 3$ ) of melphalan (A–C) or carboplatin (D–F). Cell death increased with increasing dose (A, D). For melphalan, migration increased with increasing dose (B), and proliferation was greatest at 0.4  $\mu\text{g}/\text{mL}$  (C). Migration and proliferation decreased with increasing dose for carboplatin (E, F). \* $P < 0.05$  versus control.

All animal studies were undertaken with approval of the Institutional Animal Care and Use Committee of the University of Tennessee Health Science Center under direct supervision of veterinarians and in compliance with the ARVO statement on the use of animals in research.

Each animal underwent three separate SSIOAC procedures spaced at 3-week intervals. The SSIOAC procedure and drug preparation technique used was described in a previous report.<sup>6</sup> Briefly, the right ophthalmic artery/eye was selected for treatment unless prohibited by vascular anomalies. Animals from each cohort were alternately treated to reduce the likelihood of bias in methodology and technique. Prior to each SSIOAC procedure, a baseline ophthalmic examination was performed. Real-time digital retinal images were obtained using a RETCAM (Clarity Medical Systems, Pleasanton, CA, data published previously<sup>6</sup>). The final SSIOAC for each animal was a terminal procedure during which intraocular pharmacokinetics were measured (results to be reported separately). Postmortem eyes, optic nerves,

ophthalmic arteries, and orbital vessels were harvested and submitted for histopathology. For the purposes of this report, descriptive histopathology of the ophthalmic and orbital vessels is reported herein; comprehensive, quantitative light microscopy and transmission electron microscopy studies will be reported separately.

Descriptive histopathology was gathered by enucleating the eyes under anesthesia 6 hours after the final SSIOAC. The enucleated eyes were immediately injected with 1-mL of 0.4% paraformaldehyde and placed in formalin. The animals were then euthanized and perfused with 10% formalin. The eyes were opened vertically with removal of nasal and temporal caps. The pupil–optic nerve section was embedded temporal side down. The eyes were completely sectioned, temporal to nasal, yielding approximate 500 sections per eye. The orbital vessels were inked, cut in approximate 5-mm increments, and serially sectioned yielding approximately 100 slides per vasculature tree. All slides were reviewed by the senior author (MWW).

**TABLE 1.** A Subset of the Microarray Data Illustrating the Inflammatory Response of Human Retinal Microvascular Endothelial Cells Activated by Melphalan (Carboplatin Data Not Shown)

Gene Description	Gene Symbol	UniGene ID	Log <sub>2</sub> Fold Change
Intercellular adhesion molecule-1	ICAM1	Hs.643447	0.752
Interleukin-8	IL8	Hs.624	0.846
Prostaglandin-endoperoxide synthase 2 (prostaglandin G/H synthase and cyclooxygenase)	PTGS2	Hs.196384	1.373
Epithelial membrane protein 1	EMP1	Hs.436298	0.802
Interferon, alpha-inducible protein 6	IFI6	Hs.523847	0.956
Heme oxygenase (decycling) 1	HMOX1	Hs.517581	0.632
Myxovirus (influenza virus) resistance 1, interferon-inducible protein p78 (mouse)	MX1	Hs.517307	1.087
2'-5'-Oligoadenylate synthetase 2, 69/71 kDa	OAS2	Hs.414332	0.900
Chemokine (C-X-C motif) ligand 11	CXCL11	Hs.632592	0.639
Lymphatic vessel endothelial hyaluronan receptor 1	LYVE-1	Hs.724458	0.895
Interferon-induced protein 44-like	IFI44L	Hs.724492	1.712
DEAD (Asp-Glu-Ala-Asp) box polypeptide 58	DDX58	Hs.190622	1.042
SAM domain and HD domain 1	C20orf118	Hs.580681	0.730
2'-5'-Oligoadenylate synthetase 1, 40/46 kDa	OAS1	Hs.524760	0.661
Interferon induced with helicase C domain 1	IFIH1	Hs.163173	0.633
Poly (ADP-ribose) polymerase family, member 9	PARP9	Hs.518200	0.617
Deltex 3-like (Drosophila)	DTX3L	Hs.518201	0.956

The entire microarray data set has been deposited in NCBF's Gene Expression Omnibus and is accessible through GEO Series accession number GSE34389 (<http://www.ncbi.nlm.nih.gov/geo/query/acc.cgi?acc=GSE34389>; data available in the public domain).

## RESULTS

We found significant effects on the in vitro cellular activity of the REC exposed to both melphalan and carboplatin as compared with controls (Fig. 1). There was a biphasic response of REC to increasing doses of melphalan, with 4  $\mu\text{g}/\text{mL}$  causing a five-fold increase in cell death and 0.4  $\mu\text{g}/\text{mL}$  inhibiting cell death (Fig. 1A). In addition to stimulation of DNA fragmentation at 4  $\mu\text{g}/\text{mL}$ , this dose also significantly increased REC migration (Fig. 1B) and cell proliferation in the remaining cells (Fig. 1C). Carboplatin treatment of REC

produced a significant increase in cell death at the highest dose (Fig. 1D; 1 mM, approximately one-third of the dose used in the in vivo model [2.69 mM or 30 mg/30 mL]), while the lowest doses of carboplatin significantly increased cell migration (Fig. 1E) and proliferation (Fig. 1F).

We performed microarray analyses and ELISA assays on REC treated for 24 hours with 4  $\mu\text{g}/\text{mL}$  melphalan or 1 mM carboplatin versus untreated cells. A large number of genes related to inflammation were activated following melphalan exposure (Table 1). Of particular interest in the setting of inflammation, was the upregulation of IL-8 and ICAM-1 genes,

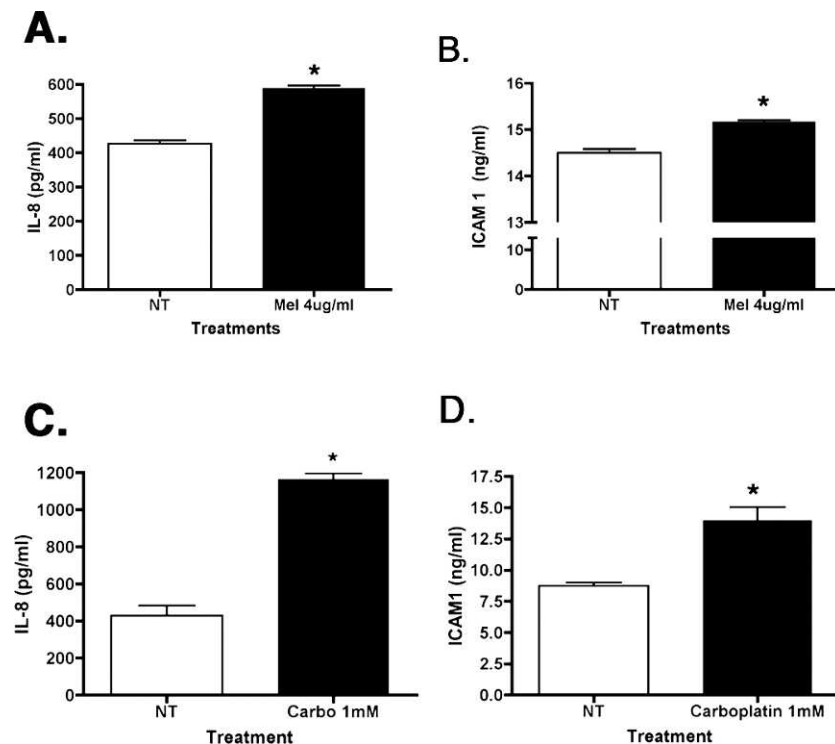


**FIGURE 2.** Increased production of adhesion genes IL-8 (in pg/mL) and ICAM-1 (in ng/mL) after treatment with 4  $\mu\text{g}/\text{mL}$  melphalan for 24 hours (A, B) or 1 mM carboplatin for 24 hours (C, D). \* $P < 0.05$  versus control (NT). NT, not treated.

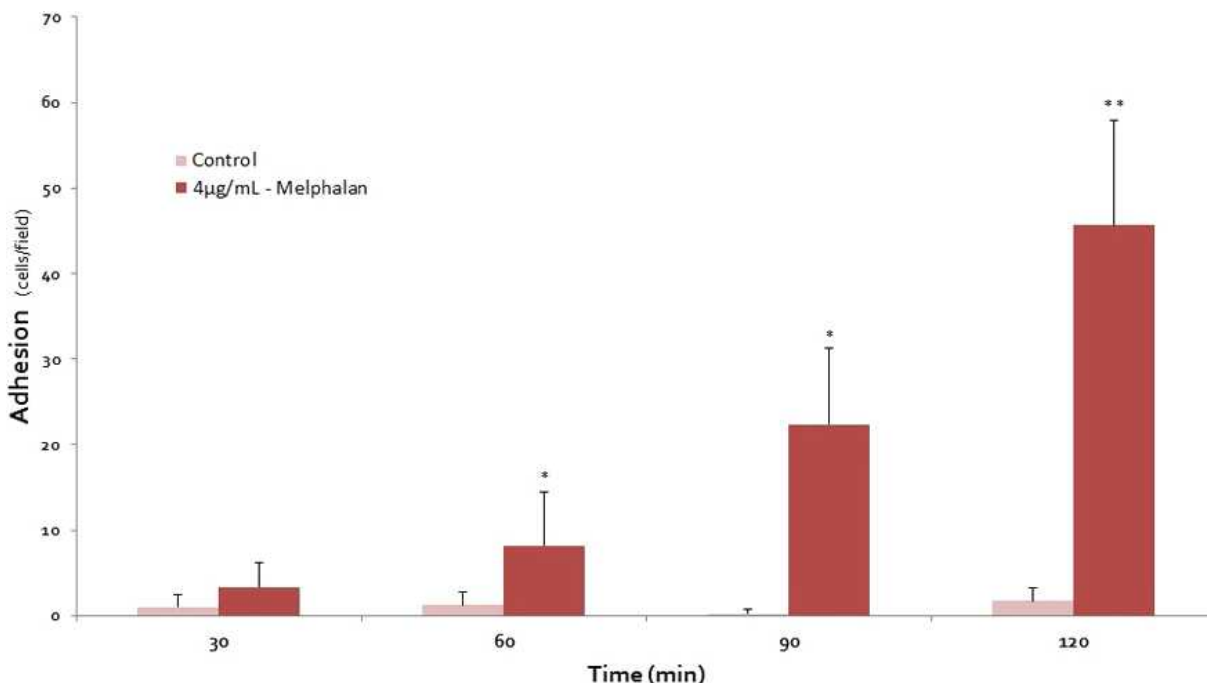


**FIGURE 3.** Flow chamber adhesion analysis. Monocytes perfused over retinal endothelial cell monolayer were analyzed over 120 minutes in the absence (light red) or presence (dark red) of melphalan (4 µg/mL). Data in 30-minute increments are expressed as the mean number of adhering cells/field ± SD for at least four different fields of view. Adhesion was significantly increased after melphalan exposure compared with control. \**P* < 0.05; \*\**P* < 0.005.

which led to significantly increased levels of IL-8 (Fig. 2A) and ICAM-1 (Fig. 2B) proteins. Carboplatin treatment also showed significant increases in the production of IL-8 (Fig. 2C) and ICAM-1 (Fig. 2D) in REC.

To evaluate whether the ICAM-1 was involved in cellular adhesion, we used a parallel plate flow chamber assay to examine the functional significance of the melphalan-induced

expression of adhesion (ICAM-1) proteins by REC. As shown in Figure 3, when U937 cells were perfused over untreated RECs at a rate of 2 dynes/cm<sup>2</sup>, negligible monocyte adhesion was observed. Conversely, the addition of 4 µg/mL melphalan in the perfusate triggered a statistically significant increase in monocyte adhesion, which began as early as 30 minutes after melphalan addition. Additionally, confocal imaging (Fig. 4) of

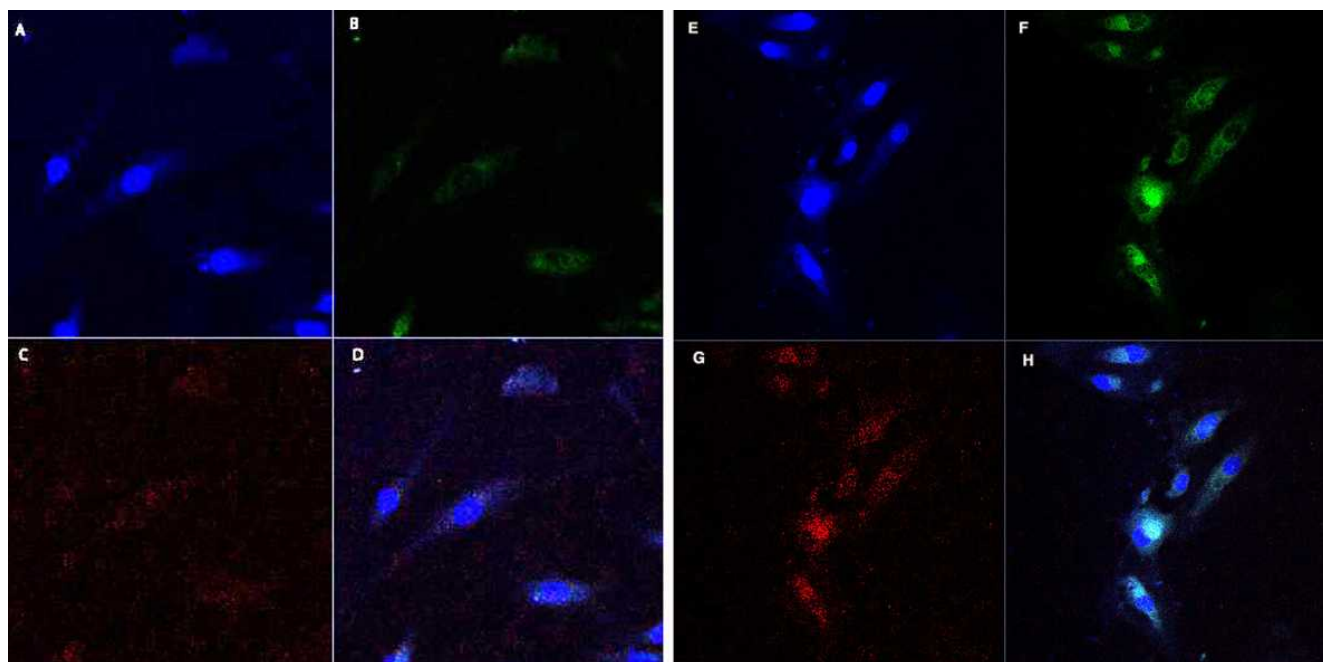


**FIGURE 4.** Representative images of control retinal endothelial cells with no treatments: (A) DAPI nuclear stain, (B) P-selectin, (C) ICAM-1, (D) overlay. Representative images of retinal endothelial cells treated with melphalan (4 µg/mL) for 2 hours: (E) DAPI nuclear stain, (F) P-selectin, (G) ICAM-1, and (H) overlay.

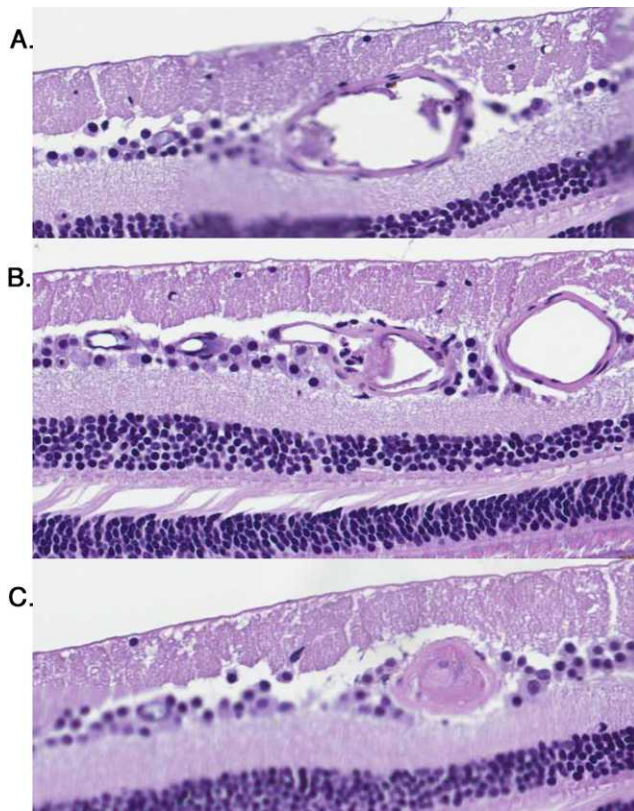


**FIGURE 5.** Serial sections of the same macular blood vessels in the ganglion cell layer (nasal to temporal) showing a progression of smudging of the endothelial cells and their basement membrane (A), with associated leukostasis (B), and terminal vessel occlusion (C).

REC exposed to melphalan showed increased expression of both P-selectin (Fig. 4F) and ICAM-1 (Fig. 4G), which is consistent with the results of the flow chamber and protein testing.

In the NHP model, descriptive histopathology analyses (Fig. 5) revealed that SSIOAC with melphalan and carboplatin produced retinal and choroidal vasculature toxicity. Serial sections of retinal arterioles, 50 to 10  $\mu\text{m}$  in diameter, revealed smudging of the endothelial cells and their basement membrane (Fig. 5A) with associated leukostasis (Fig. 5B) and terminal vessel occlusion (Fig. 5C) in the six animals, regardless of chemotherapeutic used. Similar changes were also seen in the short posterior ciliary arteries and choroidal vessels, which were slightly larger in diameter, 60 to 90  $\mu\text{m}$ .

## DISCUSSION

SSIOAC has come to the forefront in the management of retinoblastoma, but ocular and orbital toxicities are now being delineated.<sup>5</sup> We undertook parallel *in vitro* and *in vivo* lines of research to determine if SSIOAC can be improved to obviate vascular side effects and provide needed treatment with appropriate drugs.

Studies have shown that both melphalan<sup>7</sup> and carboplatin<sup>8</sup> are effective in killing retinoblastoma cells at the doses used here, but little has been done to investigate whether either drug is toxic to normal ocular elements in concentrations being used for SSIOAC. At the highest concentrations studied *in vitro*, both drugs produced a five-fold increase in cell death of REC compared with controls and also triggered cellular migration and proliferation in the surviving cells. Protein

analyses and mRNA of REC exposed to melphalan and carboplatin for 24 hours showed a significant increase in multiple inflammatory mediators, particularly IL-8 and ICAM-1. Increased expression of these molecules is consistent with our observation that treatment of REC with melphalan *in vitro* increases adhesion of monocytes to REC monolayers.

In breast cancer cells, inhibition of IL-8 can decrease cellular migration and invasion,<sup>13</sup> suggesting that IL-8 is key to cell migration in other cancer cell types. In nude mice with altered retinoblastoma gene levels, IL-8 increased neutrophil migration in the retinoblastoma-competent cells versus retinoblastoma-defective cells.<sup>14</sup> Work in the liver using the ischemia-reperfusion model has shown that the use of antibodies against ICAM-1 can prevent leukostasis and neutrophil adherence.<sup>15</sup>

For our *in vivo* studies, we chose to use an NHP model (Rhesus macaques; *Macacca mulatta*). Although our NHP model does not completely mimic a child with retinoblastoma—our treated eyes were devoid of pathology with an intact blood-retinal barrier—it approximates the weight and size of an average 2-year-old child with a comparable orbital vascular anatomy, and an eye of similar size and anatomy. We can therefore conclude that the drug distribution from the ostium of the ophthalmic artery, through the central artery, to the choroid and retina is analogous; thus our observed vascular toxicities are relevant to children treated via SSIOAC. Although others have used a porcine model, the marked vascular and ocular anatomical differences favor an NHP model.<sup>16,17</sup> Our studies were exploratory in nature and as such are subject to limitations. Our NHP cohort was limited to six animals. We felt it best to treat each animal in accordance with the literature to ensure our findings were reproducible, which they proved to be. After the first two infusions (of 18 total), each infusion included a 5-minute infusion of normal saline prior to treatment; no animal was treated with vehicle alone. Other than variations in optic nerve appearance, we saw no vascular toxicities during the pre-infusion.

In contrast to melphalan, which was previously used primarily as a high-dose alkylator for bone-marrow ablation prior to bone-marrow transplants<sup>18</sup> and to treat multiple myeloma,<sup>19</sup> there is extensive experience with carboplatin in the treatment of intraocular retinoblastoma. Although periocular delivery has demonstrated therapeutic intraocular levels of carboplatin,<sup>20</sup> the principle route of delivery has been intravenous in conjunction with vincristine and etoposide.<sup>21</sup> We are unaware of similar vascular toxicities reported with intravenous administration of carboplatin. As both melphalan and carboplatin elicited similar *in vitro* and *in vivo* responses, the clinical response recently seen to SSIOAC with melphalan<sup>4,6</sup> may be a result of one or several of the following mechanisms: pH of infusate, mechanical stress, and/or particle size (of the chemotherapeutic drug).

Both melphalan and carboplatin are typically dissolved in saline at pH 5.0 to 5.5, making the solutions relatively acidic. Nonetheless, the treatments are vastly diluted when introduced into large-caliber venous vessels. The effect of infusing an acidic solution into a small-caliber artery, such as the ophthalmic artery, is not known. Given the strong precedent for acid-induced toxicities in other vascular conditions such as thrombophlebitis,<sup>22</sup> there is a clear need to further determine if toxicity, drug solubility, and efficacy could be altered by use of pH-adjusted or buffered infusion solutions.

Another consideration is that pulsatile SSIOAC infusion may produce mechanical stress to the ophthalmic artery, the central retinal artery, as well as the small vessels of the retina and choroid, and may cause blunt trauma to the endothelial cells or pericytes. The preliminary studies reported here did not include a cohort of SSIOAC infusions with the only vehicle, normal saline. Such a cohort would help determine if

mechanical damage caused by the SSIOAC process itself is occurring; this cohort is planned for future studies.

Finally, studies in atherosclerosis on medium to large vessels have demonstrated that microvesicles, much smaller than the diameter of melphalan precipitate seen in our real-time RETCAM studies (approximately 5  $\mu\text{m}$ ),<sup>6</sup> trigger increased adhesion to the vascular wall of the blood vessels, along with increased ICAM-1 expression in the endothelial cells of the blood vessels.<sup>23</sup> The expression of inflammatory adhesion markers, such as ICAM-1, can be regulated by flow factors such as wall shear rate, particle size, and blood composition.<sup>24,25</sup>

Taken together, the pulsatile flow created by manual control of infusion, coupled with formation of precipitated material seen in our previous report,<sup>6</sup> could be expected to create an environment capable of triggering an inflammatory response leading to leukostasis and eventually to the types of retinal arteriole emboli, or Roth Spots, observed in human subjects.<sup>4</sup>

In conclusion, using SSIOAC to deliver clinical doses of either melphalan or carboplatin in an NHP model resulted in ocular vascular toxicities in exploratory studies. In human REC treated with much lower doses of melphalan or carboplatin, cell death was increased significantly, while surviving cells had increased cell migration and proliferation compared with diluent-only treatment. The increase in cell migration and proliferation was associated with increased mRNA and protein levels of IL-8 and ICAM1, which corresponded to increased neutrophils observed in retinal vessels in vivo. Future work will optimize SSIOAC to address pH, pulsatile delivery, and optimal drug of choice.

## References

- Abramson DH, Dunkel IJ, Brodie SE, Kim JW, Gobin YP. A phase I/II study of direct intraarterial (ophthalmic artery) chemotherapy with melphalan for intraocular retinoblastoma initial results. *Ophthalmology*. 2008;115:1398-1404.
- Gobin YP, Dunkel IJ, Marr BP, Brodie SE, Abramson DH. Intra-arterial chemotherapy for the management of retinoblastoma: four-year experience. *Arch Ophthalmol*. 2011;129:732-737.
- Samuels BL, Bitran JD. High-dose intravenous melphalan: a review. *J Clin Oncol*. 1995;13:1786-1799.
- Munier FL, Beck-Popovic M, Balmer A, Gaillard MC, Bovey E, Binaghi S. Occurrence of sectoral choroidal occlusive vasculopathy and retinal arteriolar embolization after superselective ophthalmic artery chemotherapy for advanced intraocular retinoblastoma. *Retina*. 2011;31:566-573.
- Shields CL, Bianciotto CG, Jabbour P, et al. Intra-arterial chemotherapy for retinoblastoma: report no. 2, treatment complications. *Arch Ophthalmol*. 2011;129:1407-1415.
- Wilson MW, Jackson JS, Phillips BX, et al. Real-time ophthalmoscopic findings of superselective intraophthalmic artery chemotherapy in a nonhuman primate model. *Arch Ophthalmol*. 2011;129:1458-1465.
- Inomata M, Kaneko A. Chemosensitivity profiles of primary and cultured human retinoblastoma cells in a human tumor clonogenic assay. *Jpn J Cancer Res*. 1987;78:858-868.
- Laurie NA, Gray JK, Zhang J, et al. Topotecan combination chemotherapy in two new rodent models of retinoblastoma. *Clin Cancer Res*. 2005;11:7569-7578.
- Wagers AJ, Waters CM, Stoolman LM, Kansas GS. Interleukin 12 and interleukin 4 control T cell adhesion to endothelial selectins through opposite effects on alpha1, 3-fucosyltransferase VII gene expression. *J Exp Med*. 1998;188:2225-2231.
- Lawrence MB, McIntire LV, Eskin SG. Effect of flow on polymorphonuclear leukocyte/endothelial cell adhesion. *Blood*. 1987;70:1284-1290.
- McCarty OJ, Mousa SA, Bray PE, Konstantopoulos K. Immobilized platelets support human colon carcinoma cell tethering, rolling, and firm adhesion under dynamic flow conditions. *Blood*. 2000;96:1789-1797.
- Alon R, Fuhlbrigge RC, Finger EB, Springer TA. Interactions through L-selectin between leukocytes and adherent leukocytes nucleate rolling adhesions on selectins and VCAM-1 in shear flow. *J Cell Biol*. 1996;135:849-865.
- Wu K, Katiyar S, Li A, et al. Dachshund inhibits oncogene-induced breast cancer cellular migration and invasion through suppression of interleukin-8. *Proc Natl Acad Sci U S A*. 2008;105:6924-6929.
- Zhang H, Wei S, Sun J, Coppola D, et al. Retinoblastoma protein activation of interleukin 8 expression inhibits tumor cell survival in nude mice. *Cell Growth Differ*. 2000;11:635-639.
- Natori S, Fujii Y, Kurosawa H, Nakano A, Shimada H. Prostaglandin E1 protects against ischemia-reperfusion injury of the liver by inhibition of neutrophil adherence to endothelial cells. *Transplantation*. 1997;64:1514-1520.
- Morén H, Gesslein B, Undrén P, Andreasson S, Malmsjö M. Endovascular coiling of the ophthalmic artery in pigs to induce retinal ischemia. *Invest Ophthalmol Vis Sci*. 2011;52:4880-4885.
- Schaiquevich P, Buitrago E, Ceciliano A, et al. Pharmacokinetic analysis of topotecan after superselective ophthalmic artery infusion and periocular administration in a porcine model [published online ahead of print July 28, 2011]. *Retina*. doi: 10.1097/IAE.0b013e31821e9f8a.
- Ninane J, Baurain R, de Selys A, Trouet A, Cornu G. High dose melphalan in children with advanced malignant disease: a pharmacokinetic study. *Cancer Chemother Pharmacol*. 1985;15:263-267.
- Oregon Health and Science University Knight Cancer Institute. Melphalan with BBBD in treating patients with brain malignancies [Clinicaltrials.gov Identifier NCT00253721]. ClinicalTrials.gov Web site. Available at: <http://www.clinicaltrials.gov/ct2/show/NCT00253721?term=NCT00253721&rank=1>. Accessed January 24, 2011.
- Abramson DH, Frank CM, Dunkel IJ. A phase I/II study of subconjunctival carboplatin for intraocular retinoblastoma. *Ophthalmology*. 1999;106:1947-1950.
- Chan HS, Gallie BL, Munier FL, Beck Popovic M. Chemotherapy for retinoblastoma. *Ophthalmol Clin North Am*. 2005;18:55-63, viii.
- Fonkalsrud EW, Murphy J, Smith FG Jr. Effect of pH in glucose infusions on development of thrombophlebitis. *J Surg Res*. 1968;8:539-543.
- Charoenphol P, Mocherla S, Bouis D, Namdee K, Pinsky DJ, Eniola-Adefeso O. Targeting therapeutics to the vascular wall in atherosclerosis—carrier size matters. *Atherosclerosis*. 2011;217:364-370.
- Charoenphol P, Huang RB, Eniola-Adefeso O. Potential role of size and hemodynamics in the efficacy of vascular-targeted spherical drug carriers. *Biomaterials*. 2010;31:1392-1402.
- Harris CA, Resau JH, Hudson EA, West RA, Moon C, McAllister JP 2nd. Mechanical contributions to astrocyte adhesion using a novel in vitro model of catheter obstruction. *Exp Neurol*. 2010;222:204-210.